

Assessment of Slow Deformations and Rapid Motions by Radar Interferometry

**RICHARD BAMLER, BERT KAMPES, NICO ADAM, STEFFEN SUCHANDT,
Oberpfaffenhofen**

ABSTRACT

Space-borne Synthetic Aperture Radar (SAR) interferometry is a powerful tool for measuring movements on ground by exploiting phase differences of SAR images taken at different time instances. Two technologies and their applications are described: 1) The persistent scatterer technique uses stacks of typically 100 images taken over up to 10 years for assessing slow deformation processes, e.g. land subsidence, at an accuracy of better than 1mm/year. 2) Along-track interferometry is used to measure the velocity of vehicles for traffic monitoring. The potential of TerraSAR-X, the German radar satellite to be launched in 2006, for interferometry is discussed.

1. SAR INTERFEROMETRY

Synthetic Aperture Radar (SAR) interferometry (InSAR) exploits the phase differences of two or more complex-valued SAR images of the same area for information extraction about topography, temporal stability, or motion (for an InSAR review see, e.g. Bamler et al., 1998). A digital surface model can be generated using the across-track InSAR configuration, i.e. where the two images are taken by SARs spatially separated in the across-track direction by typically a few hundred meters (spatial baseline). Monitoring movements requires images taken at different time instances (temporal baseline). In the paper we will discuss two extremes: 1) the assessment of slow deformation processes, e.g. land subsidence, and 2) rapid motion measurements for traffic monitoring. In the first application up to hundred images spanning a period of about 10 years are used, while for the latter application the time lag of the images is less than a millisecond.

2. PERSISTENT SCATTERER INTERFEROMETRY (PSI)

The observed phase at a pixel in an interferogram is related to the difference in measured distances of a terrain element to the radar sensors at the times of the acquisitions. This difference in turn is a mixture of displacement, topography, and atmospheric delay. In most InSAR applications it is assumed that the component of interest is dominantly present, while the other contributions can either be estimated independently or practically neglected. Moreover, in most studies the coherence of the interferogram (i.e., the precision of the phase observations) is relatively high, supporting interpretation. However, due to temporal and geometrical decorrelation (see, e.g., Gatelli et al., 1994; Zebker et al., 1992), high coherence can not be expected in general, and long-term observations by traditional InSAR techniques are therefore often restricted to non-vegetated areas.

In the late 1990s, the multi-image Permanent Scatterer (PS) technique was introduced (Ferretti et al., 1999). This technique offers a systematic processing strategy, capable of utilizing all archived data of a certain area, by creating a stack of differential interferograms that have a common master image. Instead of analyzing the phase in the spatial domain, the phase of isolated coherent points is analyzed as a function of time and space. A detailed description of the PS technique can be found in (Colesanti et al., 2003a,b; Ferretti et al., 2000, 2001). The PS technique bypasses the problem of geometrical and temporal decorrelation by considering only point-like scatterers. Furthermore, by using a large amount of data, the atmospheric signal is estimated and corrected for. It offers a con-

venient processing framework that enables the use of all acquired images (irrespective of baseline), and a parameter estimation strategy for interferograms with low spatial coherence.

Once the PS technique had demonstrated that using a large number of images was a way to reduce atmospheric artifacts and to obtain highly precise estimates despite decorrelation, this sparked the development of a number of related techniques, e.g., Coherent Target Monitoring, Interferometric Point Target Analysis, Stable Point Network Analysis, Small Baseline Subset Approach, and Corner Reflector Interferometry. These techniques partly seek to improve the PS technique using modified approaches, but also partly try to avoid disputes over the patent of the PS technique. The term Persistent Scatterer Interferometry (PSI) is now used to group techniques that analyze the phase of long-time coherent scatterers.

At DLR, the existing operational GENESIS (Generic SAR interferometric software) system has been extended with PSI processing capability (Adam et al. 2003, 2004).

2.1. The PSI estimation algorithm

A general description of the PSI-GENESIS system is given in (Kampes and Adam, 2004). The novel displacement estimation algorithm used in the system is called “Spatio-Temporal Unwrapping Network” (STUN). The three-dimensional unwrapping of the observed wrapped data in the generated interferometric stack is based (i) on a parametric temporal displacement model and (ii) on spatial unwrapping. The displacement can be modeled by a constant rate, but this estimator is easily extended to more complex displacement models, mainly because the integer ambiguity space is searched, and not the solution space of the displacement parameters. The STUN algorithm is described in detail in (Kampes, 2005). Key points are:

The displacement is modeled for each stable scatterer using a linear combination of base functions. The coefficients of these base functions are estimated simultaneously with a topographic term, and, if desired, with terms accounting for the average atmospheric delay and the sub-pixel position of the PS point.

The integer least-squares estimator is used, see (Kampes and Hanssen, 2004). The estimator is routinely used for resolving phase ambiguities of GPS observations, and has been adapted to the PSI case.

A variance components stochastic model is used to weight the observations. This model accounts for random noise and varying atmospheric signal during the acquisition times.

A variance components estimation is performed using the so-called PS candidates to obtain estimates for the precision of the double-differenced (in time and space) phase observations used during the parameter estimation.

Alternative hypothesis tests are performed to identify incorrect estimations and to guarantee a consistent network.

The sparse grid Minimum Cost Flow phase unwrapping algorithm (Eineder and Holzner, 1999) is applied, and the unwrapped data are used during the final estimation.

The variance-covariance matrix of the estimated parameters is obtained, describing the precision of and correlation between the estimated parameters.

2.2. Subsidence Monitoring

PSI processing is particularly useful for the analysis of urban displacements, because many man-made objects have perpendicular edges or are metallic, which are likely to act as stable point-scatterers. Since the data of the ERS satellites are archived since 1992, PSI is a very practical tool to obtain information on these displacements, using these historic data.

DLR's GENESIS-PSI system was used in the course of an ESA study on a test site near Marseille, France, which included rural and mountainous terrain. In this test site, mining activities have led to surface subsidence. The displacement can be modeled by a linear displacements rate in this case. For the analysis, 79 ERS-1 and ERS-2 acquisition are used spanning from May 6, 1992, through October 25, 2003. The master image of the stack was acquired on March 20, 1999. The processed area is approximately 25 km by 40 km.

The first step of the STUN algorithm is to estimate the error of the observed data. It is propagated to the error of the estimated parameters. The correlation between the estimated parameters can be neglected in this case, the correlation coefficient is 0.03. The estimated standard deviation of the estimated topographic term is as low as ~ 0.33 m and ~ 0.19 mm/y for the estimated linear displacement rate. These values are valid for relative estimations between points ~ 1500 m apart, and get larger for points further away, due to an increasing atmospheric difference signal with distance. Figure 1 shows the estimated linear displacement rates. In general, the processed area is stable, except the deforming area in the center with maximum average subsidence rates of ~ 13 mm/y for the observed time interval. The detected points lie in a network of opportunity, i.e., their location depends on the stability of the radar signature of the objects under a range of look angles. Displacement time series are shown in figure 2 for two points close to and in the subsidence area.

2.3. Seasonal Deformation

The Las Vegas area is the second test site described in this paper. Las Vegas is one of the fastest growing metropolitan areas in the USA. Between 1990 and 2000 the population almost doubled. In the metropolitan area live ~ 1.4 million people. Currently, the urbanized area is approximately 20 km by 20 km. Las Vegas lies in a broad desert valley in southern Nevada. Mountains surrounding the valley extend to ~ 3500 m above the valley floor. The average annual precipitation varies significantly from year to year but typically is between 5 and 20 cm. The area undergoes large displacements, dominantly linear and locally seasonal of nature. The local subsidence is primarily caused by groundwater withdrawal. Between 1948 and 1963 the center of the valley had subsided ~ 1.0 m, and by 1980 ~ 1.5 m, and it still continues to do so, see also (Bell et al. 2002).

For this area, 45 ERS-1 and ERS-2 acquisitions were available from April 21, 1992, to February 18, 2000. The selected master image was acquired on June 13, 1997. Significant atmospheric signal is visible in the interferograms.

The displacement is modeled using a linear and two trigonometric base functions for describing a displacement rate with a superimposed seasonal component of a one year period. The estimated average displacement rate between 1992 and 2000 is depicted in figure 3. The background image shows the average intensity of the 45 acquisitions. The NS-EW street pattern, typical for American cities, can be clearly seen in this image, as well as highway 95 (upper left to lower right), highway 15 (center to upper right), and the mountains surrounding Las Vegas. The high subsidence rates in the subsidence bowls can also clearly be identified. Figure 4 shows the seasonal component. Clearly, the estimated amplitude of the seasonal displacement is significant for the central subsidence bowl, i.e., ~ 10 mm. Also the phase offset of the seasonal displacement has been estimated. The average estimated offset is ~ 0.5 year at the positions with the largest amplitude. Since the master image is acquired June 13, the maximum (relative uplift) of the seasonal term thus occurs around March and the minimum (additional subsidence) around September.

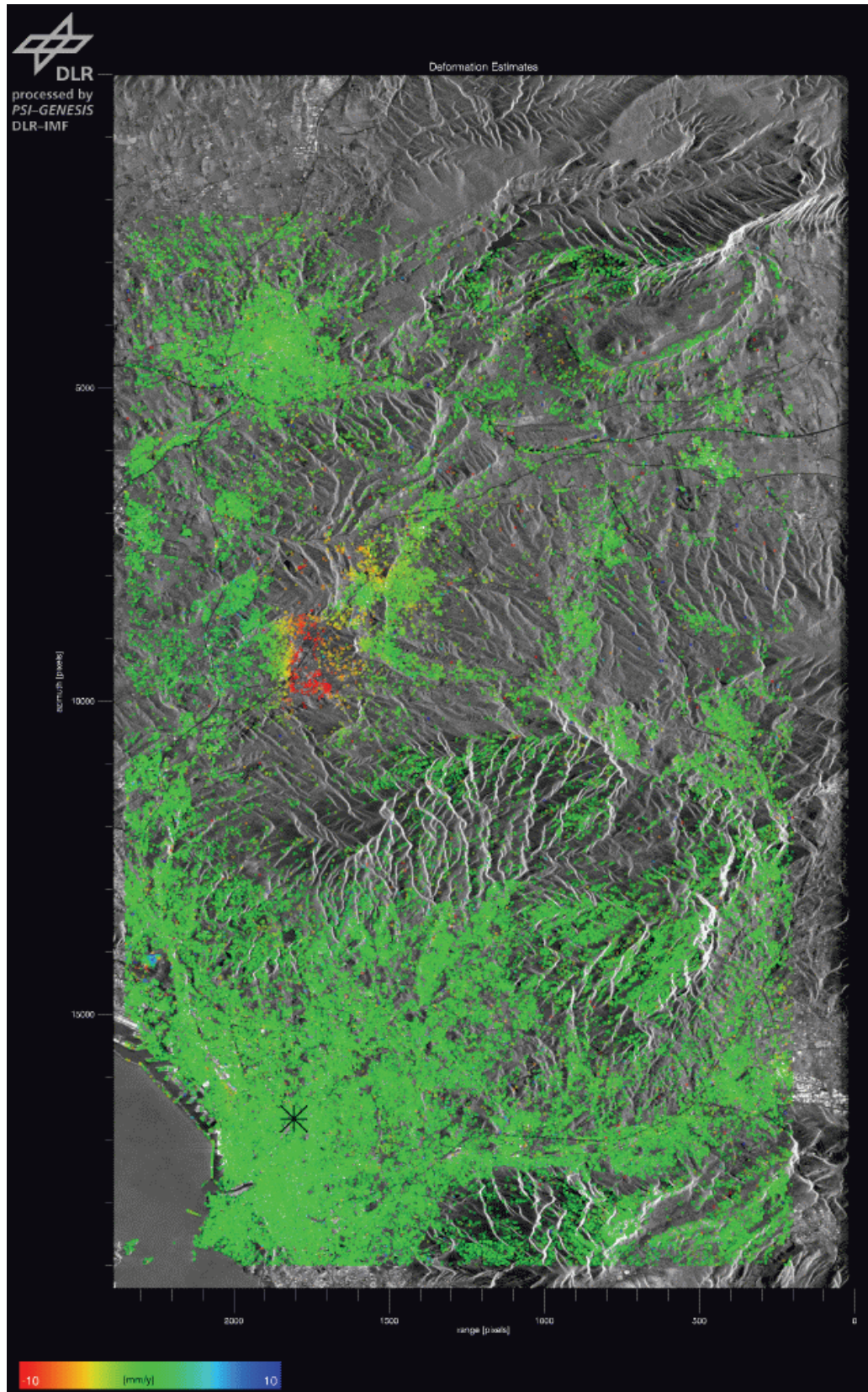


Figure 1: Estimated linear displacement rates at finally selected points using data corrected for atmospheric signal. Plotted in the range $[-10, 10]$ mm/y. Subsidence rates near the city of Gardanne of more than 10 mm/y (red) are detected.

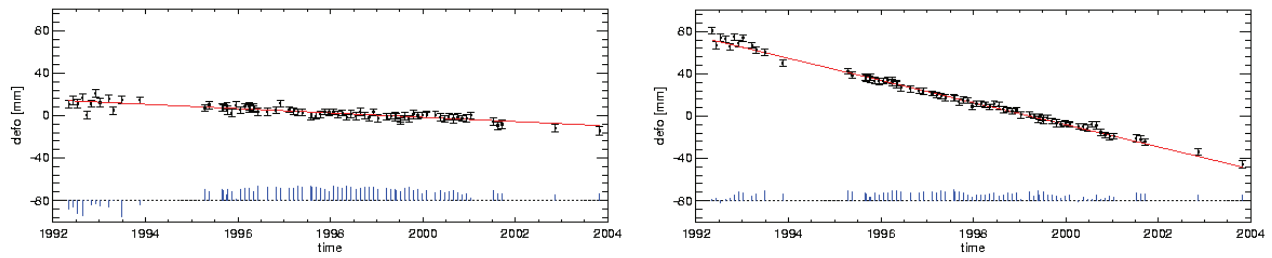


Figure 2: Displacement time series for a point near (left) and a point in (right) the subsidence area. The estimated line-of-sight displacement rates of 2.0 mm/y and 10.5 mm/y, respectively, are indicated by the red lines. The error bars show the estimated one-sigma error of ~ 3 mm. On the bottom, the amplitude time series of the PS points is given in dB.

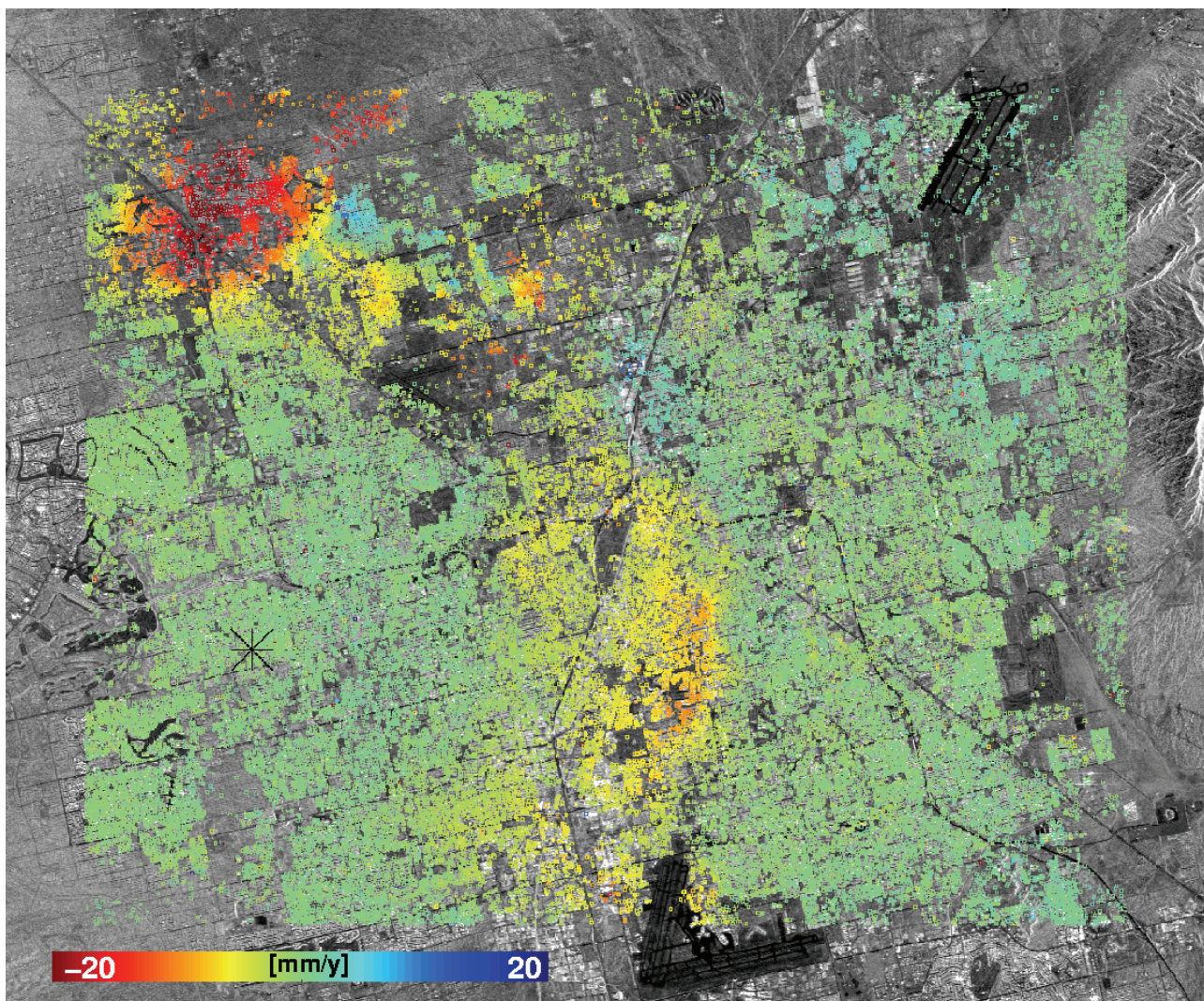


Figure 3: Estimated average displacement rate for the Las Vegas area between 1992 and 2000. Red corresponds to 20 mm/y subsidence and blue to 20 mm/y uplift. Large subsidence bowls are clearly visible, caused by ground water extraction.

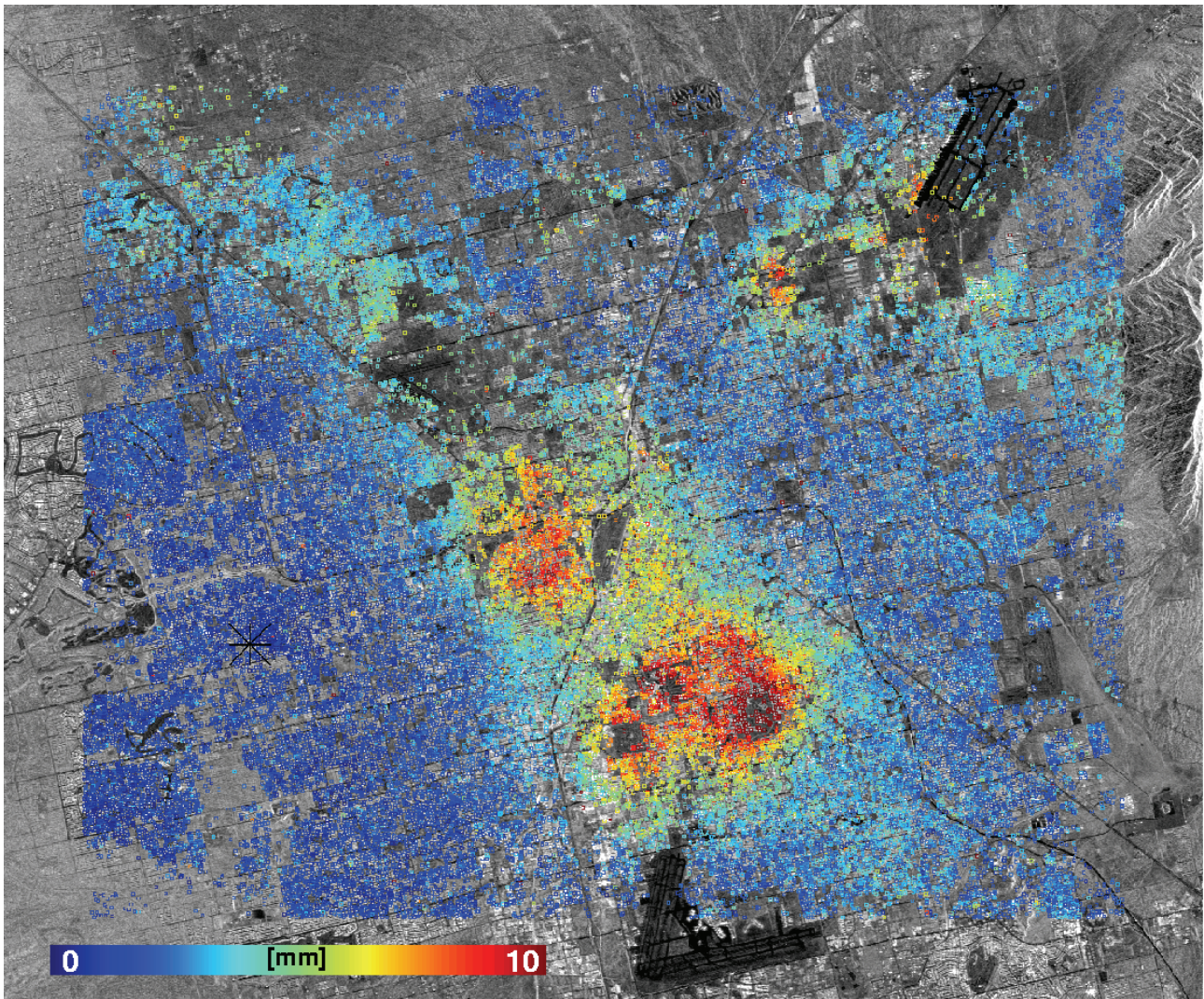


Figure 4: Estimated amplitude of seasonal displacement for the Las Vegas area. Red corresponds to 10 mm. The seasonal variation of the displacement is caused by natural and artificial recharge of the ground water reservoirs.

2.4. PSI with TerraSAR-X

TerraSAR-X, the German SAR satellite to be launched in 2006, will be optimally suited for PSI. Compared to the ERS- and ENVISAT-type data, TerraSAR-X data will exhibit the following features favorable for PSI applications:

The increase of resolution by a factor of 40 will render many more man-made and natural objects as permanent scatterers. We expect a dramatic increase of PS density, even in natural environment (e.g. landslides).

The revisit time will be 11 days and, hence, interferometric stacks can be built up three times faster. Full polarization will be available. This helps to distinguish between different scattering mechanisms (specular, double, or triple reflection).

The shorter radar wavelength will approximately double the displacement sensitivity.

3. TRAFFIC MONITORING

Due to the rapidly increasing traffic density in many parts of the world, there exists a great need for large scale acquisition of traffic data independent of weather and day time. That is why SAR interferometry for traffic monitoring has received increasing attention in recent years. Detecting and measuring moving cars with SAR techniques is usually referred to as Ground Moving Target Indication (GMTI). GMTI both exploits and suffers from the fact, that a moving object changes the SAR azimuth phase history. Since SAR focusing is based on filters matched to the signal of stationary targets, the motion of objects induces several effects to their response in the focused image such as azimuth displacements, peak reductions and ambiguities (due to across-track velocities), defocusing (due to along-track velocities and across-track accelerations) and reduced/non-symmetric target peaks (due to along-track accelerations).

Multi-channel systems like along-track interferometers (ATI) allow for a much better detection of moving objects than single channel SARs. The principle of ATI is shown in figure 5. Two SAR antennas A_1 and A_2 are separated by the baseline B_{ATI} in the flight direction. As the sensor carrier moves along the flight track at the velocity v_s , both antennas image the same area with a time lag of $\delta t = B_{ATI} / v_s$ under the look angle θ . The SAR phase is proportional to the slant range distance R_0 of the antenna to a particular ground point. In the interferogram formed from the two ATI SAR images any change of the across-track position y of a scatterer translates into an ATI phase. Hence, ATI measures the across-track motion v_y of ground objects.

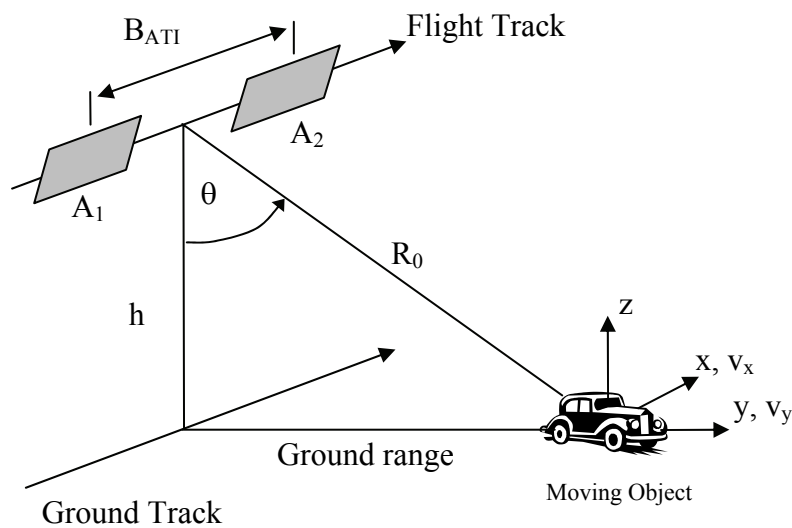


Figure 5: Principle of along-track interferometry (ATI)

3.1. TerraSAR-X Split Antenna Mode

In order to enable SAR ATI with a single satellite and without any extension like a mast, the TerraSAR-X (TS-X) antenna can be split electronically in two halves in the along-track direction. In order not to broaden the antenna pattern too much and to avoid excessive power loss, the entire antenna is used for transmission. On receive the two antenna halves are linked to two separate receiver channels. Actually for this upgrade, which has been introduced relatively late into the design of the satellite, no additional hardware was necessary. The second receiver channel already existed as redundancy. Figure 6 depicts the concept and in (Mittermayer et al., 2003) more applications of the

dual receive mode are described. The overall TS-X antenna is nearly 5 m long, which leads an along track distance between the two receive phase centers of app. 2.5 m. Due to the bi-static operation the effective along track baseline is again only one half of this value. However, the sensitivity of this relatively short ATI baseline is suited for the measurement of fast moving targets like cars.

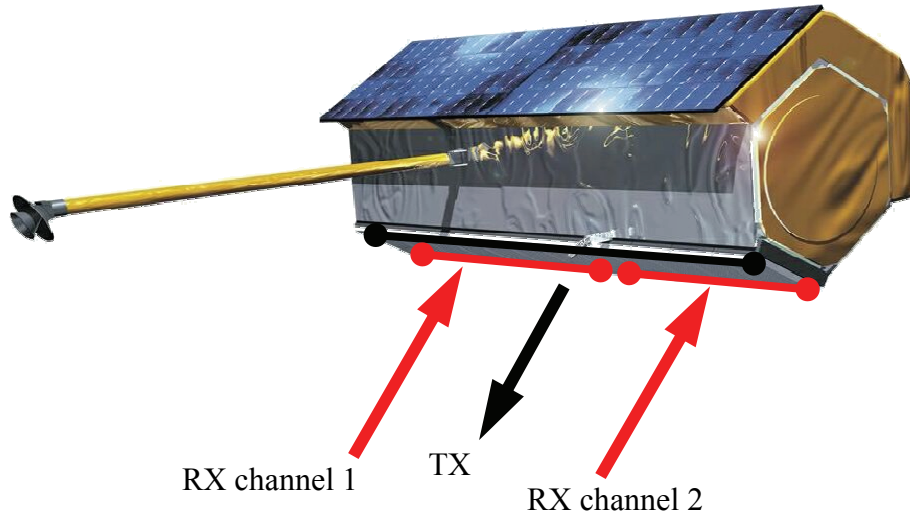


Figure 6: The radar antenna of TerraSAR-X electrically split in two halves on receive

3.2. Space Shuttle Experiment

The application of TerraSAR-X and its dual receive antenna (DRA) mode for traffic monitoring requires the theoretical and experimental investigation of space-borne sensors for GMTI. Up to now there is no civilian operational SAR satellite with ATI capability. Data from the Shuttle Radar Topography Mission (SRTM) represent the only chance to experimentally study ATI for a space-borne system. SRTM was flown from 11-22 February 2000 having the German/Italian X-SAR and the US SIR-C SAR interferometers on board the Space Shuttle Endeavour. Its main objective was to map the Earth's land mass between ± 60 degrees latitude using across-track SAR interferometry (Rabus et al., 2003). The acquired X- and C-band data were processed at the German Aerospace Center and the Jet Propulsion Laboratory, respectively, to a homogenous and highly precise Digital Elevation Model. The across-track baseline was formed by a 60 m long boom extending from the shuttle cargo bay and carrying a set of receive (RX)-only antennas on its tip. Due to mechanical restrictions the mast had to be mounted 7 m offset in flight direction with respect to the in-board antennae. By this an along-track interferometer of opportunity was formed (figure 7).

To demonstrate the capability of such a space-borne ATI instrument, an experiment was carried out during an SRTM/X-SAR data take over the area of Munich/Germany on February 18, 2000 at 10:22 AM local time (Breit et al., 2003). A car with a GPS receiver was driving on a public road while being imaged by the radar. It had been equipped with a Luneberg lens on the roof to enhance its visibility in the radar images and with GPS. Due to the 60 m across-track baseline of SRTM the resulting interferometric phase also contains contributions from topography. Nevertheless, the spatially isolated phase contributions of the moving car could be easily detected, e.g. in the coherence estimate.

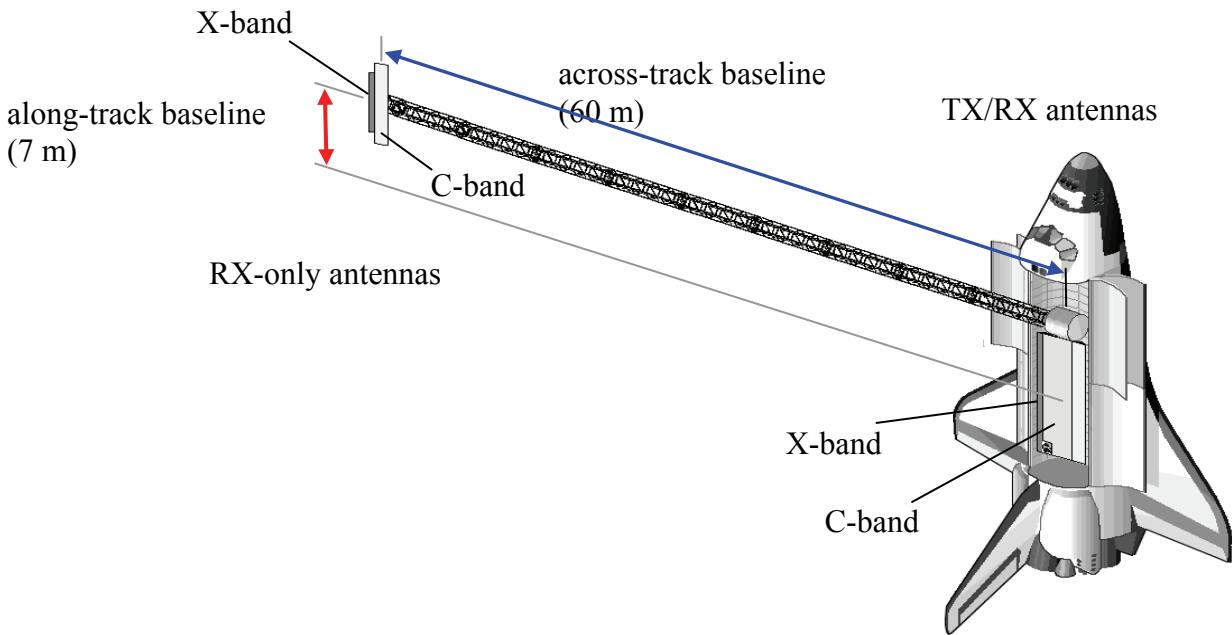


Figure 7: The interferometric configuration of SRTM. The displacement of the mast mounting away from the phase centers of the TX/RX antennas creates an along-track baseline component of 7 m.

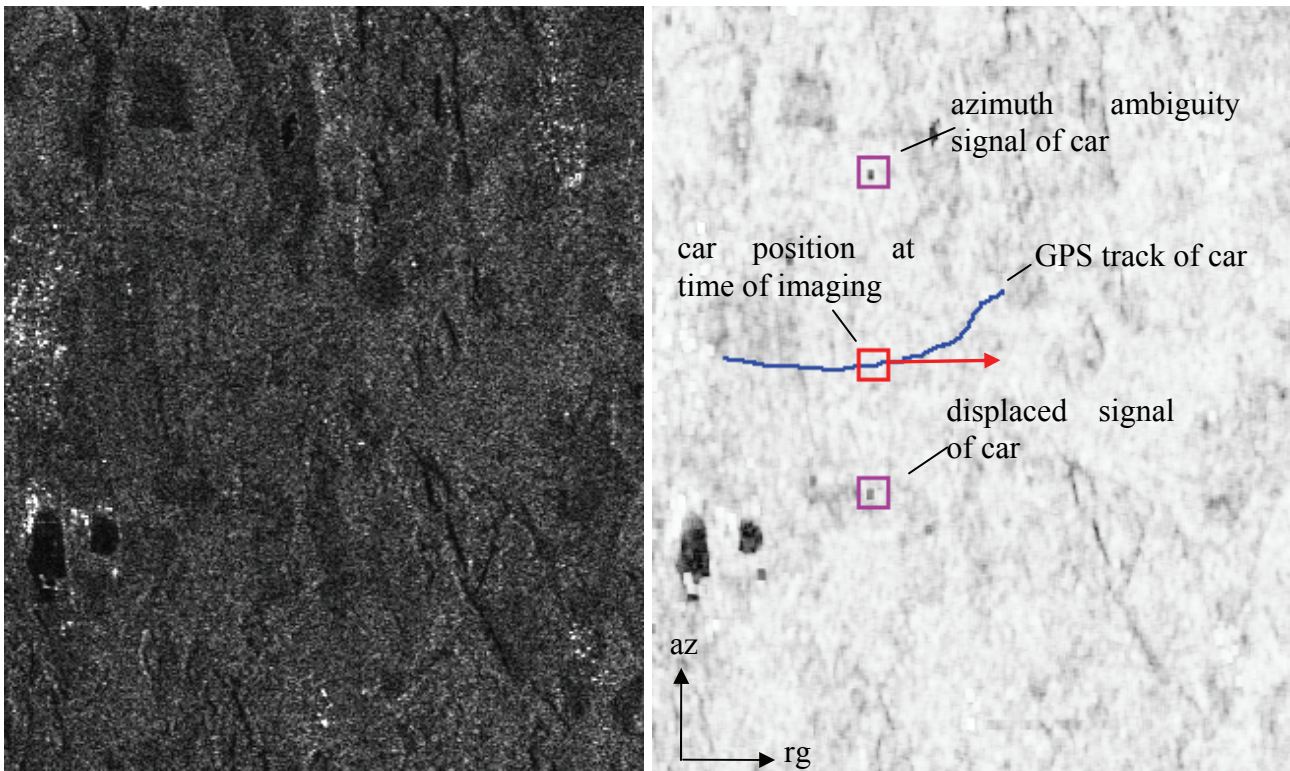


Figure 8: SAR amplitude (left) and interferometric coherence (right) of the SRTM/X-SAR GMTI experiment data take. The track of the car and its position at the time of imaging are shown in blue and red respectively. The pink boxes mark the predicted displaced positions of the car in the SAR image.

Figure 8 shows a the SAR amplitude (left) and the interferometric coherence image (right) from the experiment superimposed by the GPS track (blue) of the car. With the car velocity at that time we can predict the azimuth displacement of the car due to its line-of-sight motion component. It can be

seen that the coherence is reduced by the moving car. The point marked by the lower pink box corresponds to the displaced main peak of the car, the upper one to its azimuth ambiguity. The velocity was estimated using the azimuth displacement and the ATI phase. To utilize the interferometric phase for velocity estimation, the topographic part must be removed. It is estimated from the pixels in the vicinity of the analyzed image position. The velocity estimation results are summarized as follows:

GPS measurement:	48.1 km/h
Estimated from azimuth displacement:	47.1 km/h
Estimated from ATI phase:	47.3 km/h

3.3. Airborne SAR Measurement

Images from airborne ATI sensors represent a valuable source of data to study GMTI. DLR has been conducting several airborne SAR GMTI flight campaigns to support the system design and the development of algorithms for a traffic processor to be operated with TerraSAR-X (Palubinskas, 2004), (Meyer and Hinz 2004), (Suchandt et al. 2005). In an experiment in April 2004 several fast and slow vehicles moving on an airfield were imaged with DLR's E-SAR instrument in X-band ATI. The resolution of the acquired single-look complex images is about 1.50 m x 1.8 m. Further details of the radar system can be found in (Scheiber et al. 1999). To investigate across-track as well as along-track velocity effects, the sensor look direction was varied throughout several data takes.

The absolute velocities ranged from 2-7 km/h and from 5-90 km/h for the slow and the fast cars, respectively. All vehicles were equipped with GPS and/or dGPS receivers, some of them also with radar reflectors to enhance their detectability. An example from a data take, in which the radar look direction was equal to the car heading, is shown in figure 9. The signatures of the moving objects are the bright spots marked in the SAR amplitude image (left). Due to the across-track velocity of the cars, they appear displaced off the runway/taxiway in the azimuth direction. The image on the right shows the corresponding interferometric phase which is clearly altered at the same positions.

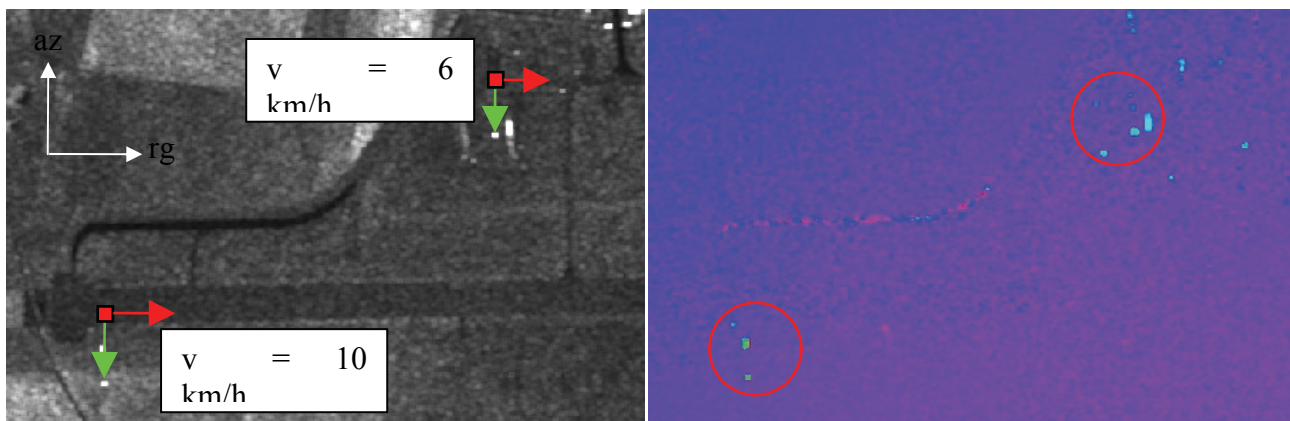


Figure 9: Data example from the airborne SAR GMTI experiment. Signals of moving cars appear in the SAR amplitude data (left). The true position and the ground velocity (red) as well as the corresponding azimuth displacement (green) have exemplarily been indicated for two cars. The right panel shows the ATI phase image. The phase signatures due to the across-track velocity of the experiment vehicles are visible in the encircled areas.

The across-track velocities of the vehicles were estimated by means of ATI phase and then projected onto the particular tracks to enable a comparison with the GPS measurements. The comparison between the velocities estimated with ATI and the true velocities of table I gives an impression of the potential accuracy of the method.

Car	ATI phase ϕ [rad]	SCR [dB]	v_{ATI} [km/h]	v_{GPS} [km/h]	Δv [km/h]
C1	-0.41	11.47	78.40	83.29	-4.89
C2	3.13	12.56	10.10	10.41	-0.31
C3	-0.81	19.75	2.35	2.27	0.08
C4	-1.02	14.15	2.93	3.79	-0.86
C5	-1.71	14.68	4.66	5.16	-0.50
C6	-2.15	19.43	6.06	6.24	-0.18

Table I: Example of velocity estimates by means of ATI phase from the E-SAR experiment.

The achievable accuracy strongly depends on the signal-to-clutter ratio (SCR) of the vehicle. It has been shown that the ATI phase gets biased towards zero as the SCR decreases (Chen, 2004). SCR can - within limits - be increased by carefully choosing imaging and processing parameters.

4. ACKNOWLEDGEMENT

ESA is acknowledged for providing data of the ERS satellite in the framework contract No. 16702/02/I-LG and 1-4594/04/I-LG.

5. REFERENCES

- Adam, N., Kampes, B. M., Eineder, M., 2004. The development of a scientific persistent scatterer system: Modifications for mixed ERS/ENVISAT time series. In: ENVISAT/ERS Symposium, Salzburg, Austria, 6-10 September, 2004, on CD-ROM.
- Adam, N., Kampes, B. M., Eineder, M., Worawattanamatekul, J., Kircher, M., 2003. The development of a scientific permanent scatterer system. In: ISPRS Workshop High Resolution Mapping from Space, Hannover, Germany, 2003, on CD-ROM.
- Bamler, R., Hartl, P., 1998. Synthetic Aperture Radar Interferometry, Inverse Problems, vol.14, pp. R1-R54.
- Bell, J. W., Amelung, F., Ramelli, A. R. and Blewitt, G., 2002. Land subsidence in Las Vegas, Nevada, 1935-2000: New geodetic data show evolution, revised spatial patterns, and reduced rates. *Geoscience and Engineering Geoscience* VIII(3), 155-174.
- Breit, H., Eineder, M., Holzner, J., Runge, H., Bamler, R., 2003. Traffic Monitoring using SRTM Along-Track Interferometry, In: Proc. of IEEE IGARSS 2003, 21-25 July, 2003, Toulouse, France.
- Colesanti, C., Ferretti, A., Novali, F., Prati, C. and Rocca, F., 2003a. SAR monitoring of progressive and seasonal ground deformation using the Permanent Scatterers Technique. *IEEE Transactions on Geoscience and Remote Sensing* 41(7), pp. 1685-1701.
- Chen, C.W., Performance Assessment of Along-Track Interferometry for Detecting Ground Moving Targets, In: IEEE Radar Conference, 26-29 April 2004, Philadelphia, U.S., Conference Proc. pp. 99-104.
- Colesanti, C., Ferretti, A., Prati, C. and Rocca, F., 2003b. Monitoring landslides and tectonic motions with the Permanent Scatterers Technique. *Engineering Geology* 68, pp. 3-14.

- Eineder, M. and Holzner, J., 1999. Phase unwrapping of low coherence differential interferograms. In: International Geoscience and Remote Sensing Symposium, Hamburg, Germany, 28 June-2 July, 1999. pp. 1-4 (cdrom).
- Ferretti, A., Prati, C. and Rocca, F., 2000. Nonlinear subsidence rate estimation using permanent scatterers in differential SAR interferometry. *IEEE Transactions on Geoscience and Remote Sensing* 38(5), pp. 2202-2212.
- Ferretti, A., Prati, C. and Rocca, F., 2001. Permanent scatterers in SAR interferometry. *IEEE Transactions on Geoscience and Remote Sensing* 39(1), pp. 8-20.
- Ferretti, A., Prati, C. and Rocca, F., 1999. Permanent scatterers in SAR interferometry. International Geoscience and Remote Sensing Symposium, Hamburg, Germany, 28 June-2 July, 1999. pp. 1-3.
- Gatelli, F., Monti Guarnieri, A., Parizzi, F., Pasquali, P., Prati, C. and Rocca, F., 1994. The wavenumber shift in SAR interferometry. *IEEE Transactions on Geoscience and Remote Sensing* 32(4), pp. 855-865.
- Kampes, B. M. and Adam, N., 2004. Deformation parameter inversion using permanent scatterers in interferogram time series. European Conference on Synthetic Aperture Radar, Ulm, Germany, 25-27 May, 2004. pp. 341-344.
- Kampes, B. M. and Hanssen, R. F., 2004. Ambiguity resolution for permanent scatterer interferometry. *IEEE Transactions on Geoscience and Remote Sensing* 42(11), pp. 2446-2453.
- Kampes, B. M., 2005. Deformation parameter estimation using permanent scatterer interferometry. PhD thesis. Delft University of Technology, Delft, The Netherlands. In press.
- Meyer, F., Hinz, S., 2004. The Feasibility of Traffic Monitoring with TerraSAR-X - Analyses and Consequences, Proc. of IEEE IGARSS 2004, 20-24 September, Anchorage, Alaska.
- Mittermayer, J., Runge, H., 2003, Conceptual Studies for Exploiting the TerraSAR-X Dual Receive Antenna, Proc. of IEEE IGARSS 2003, 21-25 July, 2003, Toulouse, France
- Palubinskas G., Runge H., Reinartz P., 2004. Radar signatures of road cars, Proc. of IEEE IGARSS, 20-24 September, 2004, Anchorage, Alaska, USA, vol. II, pp. 1498-1501.
- Rabus, B. Eineder, M., Roth, A., Bamler, R., 2003. The shuttle radar topography mission – a new class of digital elevation models acquired by spaceborne radar, *ISPRS Journal of Photogrammetry and Remote Sensing* 57, pp. 241-262.
- Scheiber, R., Reigber, A., Ulbricht, A., Papathanassiou, K.P., Horn, R., Buckreiß, S., Moreira, A., 1999. Overview of Interferometric Data Acquisition and Processing Modes of the Experimental Airborne SAR System of DLR., Proc. of IEEE IGARSS 1999, Hamburg, Germany.
- Suchandt, S., Palubinskas, G., Runge, H., Eineder, M., Meyer, F., 2005. An Airborne SAR Experiment for Ground Moving Target Identification, ISPRS Hannover Workshop 2005, "High Resolution Earth Imaging for Geospatial Information", Hannover, Germany, 17-20 May 2005, Conference Proceedings, Vol. XXXVI, ISSN No. 1682-1777, Part I/W3.
- Zebker, H. A. and Villasenor, J., 1992. Decorrelation in interferometric radar echoes. *IEEE Transactions on Geoscience and Remote Sensing* 30(5), pp. 950-959.